

# Comparison of the normal state properties of $\kappa$ -(BEDT-TTF)<sub>2</sub>Cu(NCS)<sub>2</sub> and its deuterated analogue in high magnetic fields and under high hydrostatic pressures

Tim Biggs<sup>1</sup>, Anne-Katrin Klehe<sup>1</sup>, John Singleton<sup>1,2,§</sup>, David Bakker<sup>1</sup>, Jane Symington<sup>1</sup>, Paul Goddard<sup>1</sup>, Arzhang Ardavan<sup>1</sup>, William Hayes<sup>1</sup>, John A Schlueter<sup>3</sup>, Takehiko Sasaki<sup>4</sup> and Mohamedally Kurmoo<sup>5</sup>

<sup>1</sup> Department of Physics, University of Oxford, The Clarendon Laboratory, Parks Road, Oxford OX1 3PU, United Kingdom

<sup>2</sup> National High Magnetic Field Laboratory, LANL, MS-E536, Los Alamos, New Mexico 87545, USA

<sup>3</sup> Materials Science Division, Argonne National Laboratory, Illinois 60439, USA

<sup>4</sup> Institute for Materials Research, Tohoku University, Aoba Ku, Sendai, Miyagi 9808577, Japan

<sup>5</sup> IPCMS, 23 rue du Loess, BP 20/CR, 67037 Strasbourg Cedex, France

**Abstract.** Details of the Fermi-surface topology of deuterated  $\kappa$ -(BEDT-TTF)<sub>2</sub>Cu(NCS)<sub>2</sub> have been measured as a function of pressure, and compared with equivalent measurements of the undeuterated salt. We find that the superconducting transition temperature is much more dramatically suppressed by increasing pressure in the deuterated salt. It is suggested that this is linked to pressure-induced changes in the Fermi-surface topology, which occur more rapidly in the deuterated salt than in the undeuterated salt as the pressure is raised. Our data suggest that the negative isotope effect observed on deuteration is due to small differences in Fermi-surface topology caused by the isotopic substitution.

Submitted to: *J. Phys.: Condens. Matter*

The nature of superconductivity in quasi-two dimensional crystalline organic metals is the subject of current debate in the literature [1, 2, 3, 4]. The close proximity of an antiferromagnetic to a superconducting groundstate in the temperature-pressure phase diagram has spurred theoretical suggestions of d-wave Cooper pairing mediated by antiferromagnetic fluctuations [3, 4, 5, 6, 7]. Such an idea, which implies nodes in the superconducting order parameter, is strongly supported by NMR (<sup>13</sup>C [8, 9, 10] and <sup>1</sup>H [11]), tunnelling [12], thermal conductivity [13] and magnetic penetration depth experiments [14], and by the form of the superconducting phase diagram deduced from magnetometry and NMR [15]. The coupling of Raman modes to the antiferromagnetic fluctuations has also been observed [16], suggesting interactions between the lattice and the magnetic fluctuations. On the other hand, it has been suggested that specific heat measurements may be interpreted using a BCS-like model [17]. The observed hardening of low energy, intramolecular vibrations at the superconducting transition in Raman [18, 19] and inelastic neutron scattering experiments [20] has been interpreted as further evidence for the involvement of phonons in superconductivity. However, similar phonon self-energy effects have also been observed in the non-BCS like Cuprate superconductors [21] and perhaps merely indicate very strong electron-phonon coupling.

In this context, the observation of a “negative isotope effect” in  $\kappa$ -(BEDT-TTF)<sub>2</sub>Cu(NCS)<sub>2</sub> may be of great importance [22, 23]; on replacing the terminal hydrogens of the BEDT-TTF molecule in  $\kappa$ -(BEDT-TTF)<sub>2</sub>Cu(NCS)<sub>2</sub> by deuterium, it was found that a small but consistent increase in the superconducting critical temperature  $T_c$  occurred [22, 23]. By contrast, isotopic substitutions of other heavier atoms in the BEDT-TTF molecule or in the anion layer exhibit a very small, normal isotope effect or no significant isotope effect at all, respectively [23]. We have therefore studied the changes in Fermi-surface parameters of  $\kappa$ -(BEDT-TTF)<sub>2</sub>Cu(NCS)<sub>2</sub> on deuteration using the Shubnikov-de Haas effect. Data were recorded both at ambient pressure and as a function of hydrostatic pressure. Taken in conjunction with very recent millimetre-wave magnetoconductivity experiments [26], our data suggest that it is primarily the changes in the detailed topology of the of the Fermi surface brought about by deuteration that cause the observed isotope effect. This would tend to support models for superconductivity involving pairing via electron-electron interactions [3, 4, 5, 6, 7].

The experiments involved single crystals of  $\kappa$ -(BEDT-TTF)<sub>2</sub>Cu(NCS)<sub>2</sub> ( $\sim 0.7 \times 0.5 \times 0.1$  mm<sup>3</sup>; mosaic spread  $\lesssim 0.1^\circ$ ), produced using electrocrystallization [22, 23]. In some of the crystals, the terminal hydrogens of the BEDT-TTF molecules were isotopically substituted by deuterium; we refer to these deuterated samples as d8, and conventional hydrogenated samples as h8. In order to check for extrinsic effects, independently-prepared batches of both types of crystal were made at Argonne, Strasbourg and Sendai; no extrinsic effects were found. Note that, to all intents and purposes, the crystallographic unit cells of h8 and d8 seem to be indistinguishable in size and shape [23, 24, 25].

The magnetoresistance of the samples was measured using standard 4 wire AC-techniques (frequency  $f = 15 - 180$  Hz, current  $I = 1 - 20$   $\mu$ A) [2]. Contacts were applied

to the upper and lower large surfaces of the crystals, so that the current was directed and the voltage measured in the interlayer direction; such a configuration gives a resistance which is accurately proportional to the interlayer component of the magnetoresistance,  $\rho_{zz}$  [2].

In the ambient-pressure experiments, crystals of d8 and h8 were simultaneously studied in a <sup>3</sup>He/<sup>4</sup>He cryostat which allowed rotation of the samples to all possible angles in the magnetic field [28]. The magnetoresistance was measured with the samples at many orientations in the magnetic field, so that any errors due to slight differences of mounting of the d8 and h8 crystals could be eliminated; the quasiparticle effective masses and Shubnikov-de Haas oscillation frequencies discussed below are corrected to  $\theta = 0$ , where  $\theta$  is the angle between the normal to the sample's conducting planes and the magnetic field. Temperatures were monitored using ruthenium oxide sensors, with additional checks carried out using the <sup>3</sup>He and <sup>4</sup>He vapour pressures. Quasistatic magnetic fields were provided by a 15 T superconductive magnet at Los Alamos and by the 45 T Hybrid magnet at NHMFL Tallahassee.

The high-pressure experiments were carried out on three d8 crystals using a non-magnetic piston-cylinder cell; the pressure medium was Fluorinert FC75 [27]. The exact crystal orientation with respect to the field was determined by comparison with ambient pressure data and corrections to the measured Shubnikov-de Haas frequency made accordingly [2]. The cell was placed in a large volume <sup>3</sup>He cryostat capable of temperatures down to 700 mK within a 17 T superconductive magnet at Oxford. The pressure inside the cell was determined using a manganin wire [27]. Temperatures were measured with a Pt thermometer above 50 K and a ruthenium oxide thermometer at low temperatures. All pressures quoted were measured at 4.2 K.  $T_c$  was taken to be the resistive midpoint of the normal-superconducting transition during cool down.

The left-hand side of Figure 1 shows typical low-field ambient-pressure magnetoresistance data for an h8 sample. Similar data were recorded simultaneously for a d8 sample. Shubnikov-de Haas oscillations caused by the quasi-two-dimensional  $\alpha$  pocket of the Fermi surface (see lower inset of Figure 1). are visible. At these low fields, the oscillatory magnetoresistance is much less than the non-oscillatory component, and magnetic breakdown is a relatively minor consideration [2]. Hence, the Lifshitz-Kosevich formula may be used to extract the effective mass  $m^*$  [2] from the temperature dependence of the oscillation amplitude  $A$ ; a typical fit is shown as the upper inset in Figure 1.

Data such as those in Figure 1 suggest that the  $\alpha$  Fermi-surface pockets of h8 and d8 are rather similar; as an example, the magnetic quantum oscillation frequencies of the  $\alpha$  pocket at  $\theta = 0$  were  $F_\alpha = 600 \pm 1$  T (h8) and  $F_\alpha = 597 \pm 1$  T (d8); the former is in good agreement with the accepted value [1]. Although the d8 and h8 frequencies are very close, consistently smaller values were obtained for the d8 samples, and so we believe that the stated difference is real. The corresponding  $\alpha$  pocket effective masses ( $\theta = 0$ ) are  $m^* = 3.5 \pm 0.1m_e$  (h8) and  $m^* = 3.4 \pm 0.1m_e$  (d8); the difference between the masses is around the experimental error. The average interlayer transfer integrals

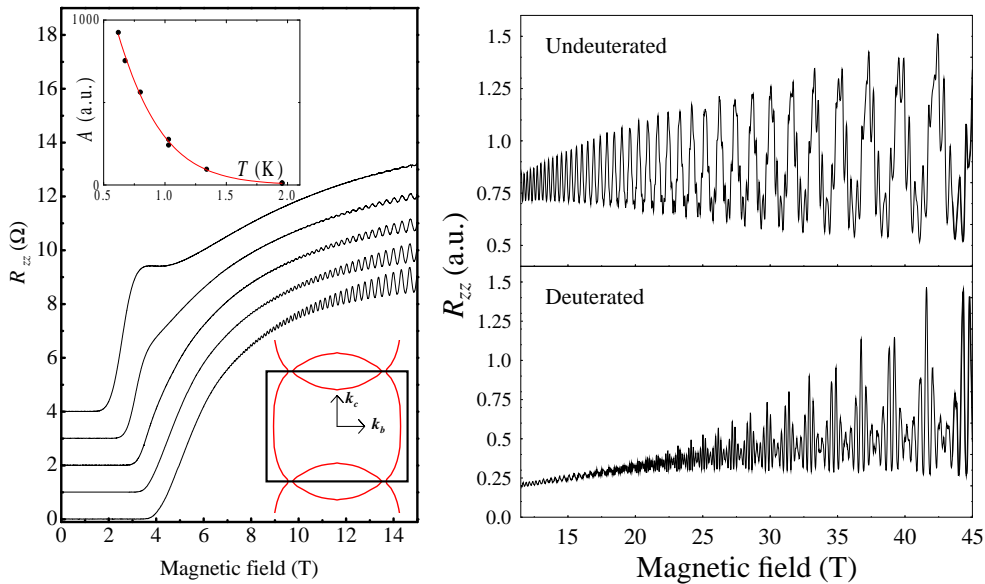


**Figure 1.** Left: interplane resistance  $R_{zz}$  ( $\propto \rho_{zz}$ ) of h8  $\kappa$ -(BEDT-TTF)<sub>2</sub>Cu(NCS)<sub>2</sub> at ambient pressure with magnetic field applied perpendicular to the quasi-two-dimensional planes. Data for temperatures 1.96 K (uppermost trace), 1.34 K, 1.03 K, 800 mK and 620 mK (lowest trace) are shown; for clarity, the data have been offset by 1  $\Omega$ . The superconducting to normal transition is clearly visible, as are Shubnikov-de Haas oscillations due to the  $\alpha$  pocket of the Fermi surface. The upper inset shows a typical plot of the Fourier amplitude  $A$  of the Shubnikov-de Haas oscillations as a function of temperature; data are points and the curve is a fit of the Lifshitz-Kosevich formula [2]. The lower inset shows the Brillouin zone and Fermi surface cross-section of  $\kappa$ -(BEDT-TTF)<sub>2</sub>Cu(NCS)<sub>2</sub> with its closed  $\alpha$  pocket and quasi-one-dimensional sheets (based on parameters given in Reference [28]). Right: comparison of the high-field interplane resistance  $R_{zz}$  of d8 (deuterated) and h8 (undeuterated)  $\kappa$ -(BEDT-TTF)<sub>2</sub>Cu(NCS)<sub>2</sub> ( $T = 520$  mK). Note how the high frequencies caused by magnetic breakdown are much more dominant in d8.

for d8 and h8 were measured in a separate experiment [28]; both were found to be very close to 0.04 meV [28].

The only significant difference between the magnetotransport of d8 and h8 at ambient pressure occurs in the magnetic breakdown between the  $\alpha$  pocket and quasi-one-dimensional sheets, which gives rise to a semiclassical orbit with the same cross-sectional area as the Brillouin zone [29]. As shown in the right-hand side of Figure 1, which displays magnetoresistance data recorded in the hybrid magnet, the breakdown is significantly stronger in d8, leading to a plethora of high frequency oscillations in the magnetoresistance due to the Shiba-Fukuyama-Stark quantum interference effect [2]. Following the method set out in Reference [29], analysis of the breakdown oscillations suggests a breakdown field of  $B_0 = 30 \pm 5$  T in d8, compared to a value of  $B_0 = 41 \pm 5$  T [29] in h8.

We now turn to the high pressure experiments. Figure 2(a) shows the pressure dependence of the effective mass  $m_\alpha^*$  of the d8  $\alpha$  Fermi-surface pocket, extracted from

the temperature dependence of the Shubnikov-de Haas oscillations [2]. At pressures of less than 0.25 GPa,  $m_\alpha^*$  decreases very sharply with increasing pressure  $P$  ( $dm_\alpha^*/dP \approx -10 m_e/\text{GPa}$ ); above this pressure, the mass decreases much more gently as  $P$  is raised. The d8 masses are compared with the h8 data of Caulfield *et al.* [30] in Figure 2(a); note that the initial rate of decrease of  $m_\alpha^*$  with  $P$  is significantly less in h8, but that the variation of  $m_\alpha^*$  is very similar in h8 and d8 at higher  $P$ .

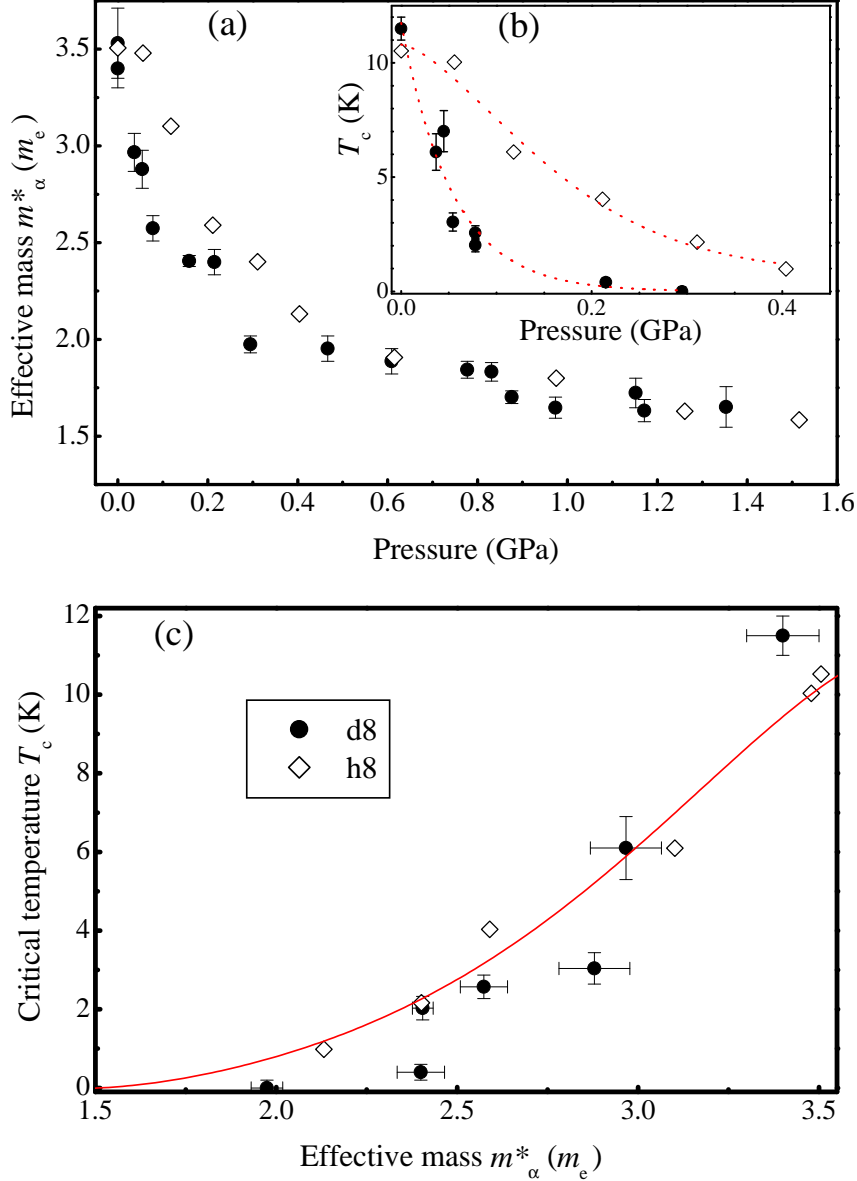


**Figure 2.** (a) Pressure dependence of the effective mass  $m_\alpha^*$  of the  $\alpha$  Fermi-surface pocket of  $\kappa$ -(BEDT-TTF)<sub>2</sub>Cu(NCS)<sub>2</sub> as a function of pressure  $P$ . Data for d8 (this work) are filled circles; data for h8 (Reference [30]) are hollow diamonds. (b) Variation of superconducting critical temperature  $T_c$  of  $\kappa$ -(BEDT-TTF)<sub>2</sub>Cu(NCS)<sub>2</sub> as a function of  $P$ ; filled circles: d8 (this work); hollow diamonds: h8 (Reference [30]). (c)  $T_c$  versus  $m_\alpha^*$  for h8 (filled circles) and d8 (hollow diamonds). The curve is the linearised Eliashberg solution from Reference [7].

Figure 2(b) shows the superconducting critical temperature  $T_c$  of  $\kappa$ -(BEDT-TTF)<sub>2</sub>Cu(NCS)<sub>2</sub> as a function of  $P$  for both d8 (this work) and h8 (Reference [30]). In the case of d8,  $T_c$  is very rapidly suppressed with increasing  $P$  ( $dT_c/dP \approx 80$  K/GPa). By contrast,  $dT_c/dP \approx 30$  K/GPa for h8 [30]. As in the case of the effective mass, the pressure seems to have a much more marked effect for d8 than for h8.

Weiss *et al.* suggested that there may be some universal relationship between  $T_c$  and  $m_\alpha^*$  in  $\kappa$ -phase BEDT-TTF superconductors [31] (see also References [30, 32]). Figure 2(c) shows such a plot for d8 (this work) and h8 (Reference [30]). Whilst the data for the two salts vary in a qualitatively similar fashion, the slope of  $T_c$  versus  $m_\alpha^*$  seems to be somewhat steeper for d8.

Figures 3(a) and (b) show the pressure dependence of the Shubnikov-de Haas oscillation frequencies for d8 and h8. As has been mentioned above, the  $\beta$ -orbit frequency  $F_\beta$  (Figure 3(b)) reflects the size of the Brillouin zone in the conducting **bc** plane; it is therefore a direct measure of the in-plane compressibility. Figure 3(b) shows that the pressure dependence of  $F_\beta$  is almost identical in h8 and d8. This suggests that any lattice softening effects due to deuteration do not affect the intraplane compressibility, and are thus, if present, only effective in the interplane direction. By contrast, the  $\alpha$  Fermi-surface pocket frequency grows much more quickly with  $P$  in d8 than in h8 (Figure 3(a)); interestingly,  $T_c$  tends to zero in *both* d8 and h8 at pressures where the  $\alpha$ -orbit frequencies reach approximately the same value,  $F_\alpha \approx 770 \pm 15$  T.

To examine the effect of pressure more deeply, we turn to the *effective dimer model* which has been shown to represent the intralayer quasiparticle dispersion  $E(\mathbf{k}_\parallel)$  in  $\kappa$ -(BEDT-TTF)<sub>2</sub>Cu(NCS)<sub>2</sub> accurately (see Reference [28] and references therein);

$$E(\mathbf{k}_\parallel) = \pm 2 \cos\left(\frac{k_{\mathbf{b}}b}{2}\right) \sqrt{t_{\mathbf{c}1}^2 + t_{\mathbf{c}2}^2 + 2t_{\mathbf{c}1}t_{\mathbf{c}2} \cos(k_{\mathbf{c}}c)} + 2t_{\mathbf{b}} \cos(k_{\mathbf{b}}b). \quad (1)$$

Here  $k_{\mathbf{b}}$  and  $k_{\mathbf{c}}$  are the intralayer components of  $\mathbf{k}$  (see Figure 1, inset) and  $t_{\mathbf{b}}$ ,  $t_{\mathbf{c}1}$  and  $t_{\mathbf{c}2}$  are effective interdimer transfer integrals [33]; the + and - signs result in the quasi-one-dimensional sheets and the  $\alpha$  pocket of the Fermi surface respectively. The cross-sectional area of the  $\alpha$  pocket is determined by the ratio  $t_{\mathbf{b}}/t_{\mathbf{c}}$ , where  $t_{\mathbf{c}}$  is the mean of  $t_{\mathbf{c}1}$  and  $t_{\mathbf{c}2}$  [28]. Using this approach [30], we can convert the frequencies  $F_\alpha$  from Figure 3(a) into values of  $t_{\mathbf{b}}/t_{\mathbf{c}}$ ; the result is shown for both h8 and d8 as the inset in Figure 3(a). The inset shows that  $t_{\mathbf{b}}/t_{\mathbf{c}}$  increases with  $P$  more rapidly in d8 than in h8.

Reference [30] shows that an increase of  $t_{\mathbf{b}}/t_{\mathbf{c}}$  elongates the overall Fermi-surface cross-section in the  $k_{\mathbf{c}}$  direction by “fattening” the  $\alpha$  pocket. As a consequence, the corrugation of the quasi-one-dimensional sheets changes somewhat; the regions next to the breakdown gap become slightly more pointed, whilst away from the gap, the sheets flatten slightly. Our data suggest that these changes occur much more rapidly with increasing pressure in d8 than in h8.

With this in mind, we suggest that the more rapid suppression of superconductivity in d8, compared to h8, is linked to the fact that the Fermi surface topology changes more drastically with pressure in d8 (Figure 3). This strongly suggests that the

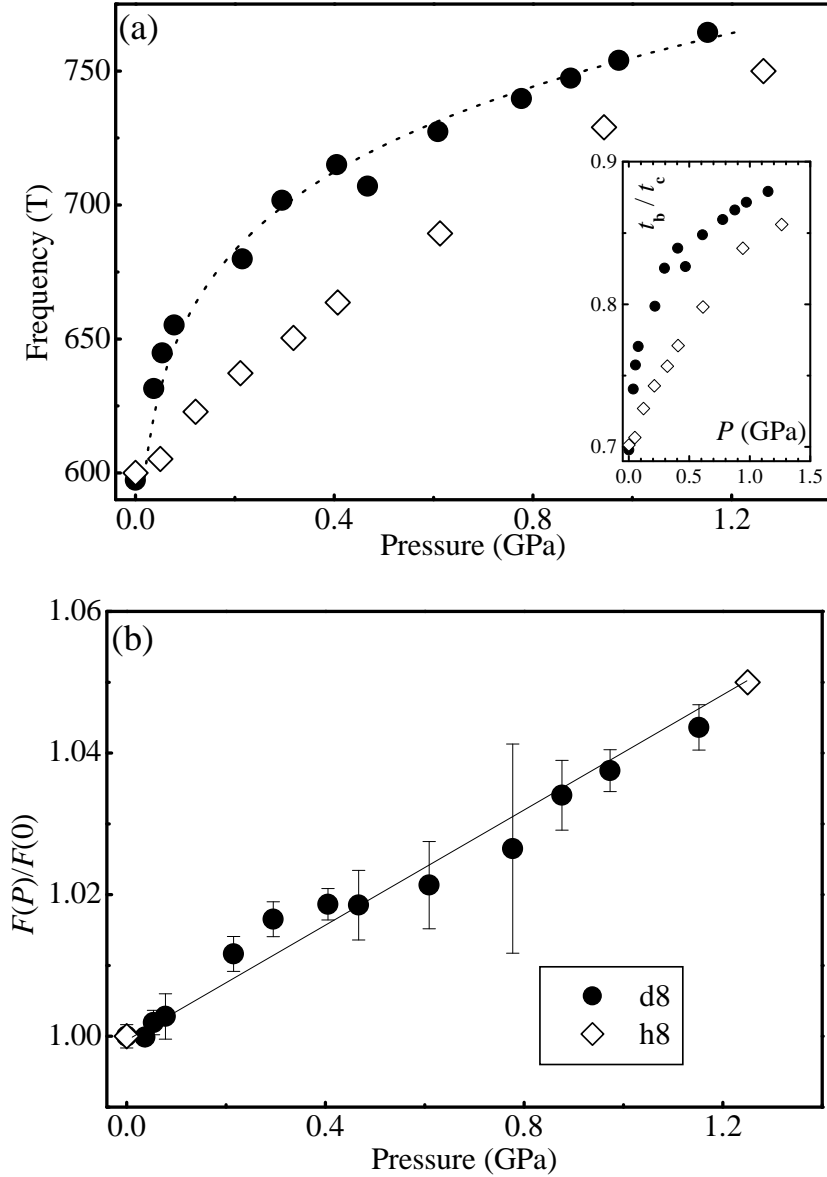


**Figure 3.** (a) Shubnikov-de Haas oscillation frequency for the  $\alpha$  Fermi-surface pocket as a function of pressure  $P$  for d8 (filled circles; this work) and h8 (hollow diamonds, Reference [30]). The inset shows  $t_b/t_c$  versus pressure, where the  $t$  are effective transfer integrals defined in Equation 1. (b) Equivalent plot for the  $\beta$  breakdown frequency, but with the frequencies normalised to the ambient-pressure value.

superconducting mechanism is very sensitively influenced by the exact topology of the Fermi surface, and hence that this effect is also responsible for the inverse isotope effect in  $\kappa$ -(BEDT-TTF)<sub>2</sub>Cu(NCS)<sub>2</sub> observed on deuteration. Additional support for this proposal is provided by the difference in magnetic breakdown strength seen in d8 and h8 at ambient pressure (Figure 1), suggesting slightly different Fermi-surface topologies for the two salts.

An alternative explanation for the inverse isotope effect invokes a softening

of the bonds upon deuteration and a concurrent increase in the electron-phonon interaction [23]. Comparative Raman studies on on deuterated and undeuterated  $\kappa$ -(BEDT-TTF)<sub>2</sub>Cu(NCS)<sub>2</sub> may also be interpreted in this way [35]. It might also be possible to simulate the size and direction of change of  $T_c$  experienced upon deuteration from the anisotropic compressibility [24, 36] of  $\kappa$ -(BEDT-TTF)<sub>2</sub>Cu(NCS)<sub>2</sub>, and the strongly anisotropic uniaxial pressure dependence of its superconducting transition temperature [37, 38, 39]. However, neither of these explanations can shed any light on the very obvious relationship between the details of the Fermi-surface shape and  $T_c$ , shown by our data (Figures 2 and 3).

Instead, our data support models for exotic d-wave superconductivity in the organics which invoke electron-electron interactions depending on the topological (i.e. nesting) properties of the Fermi surface [3, 4, 5, 6]. Similar interactions probably contribute to the relatively large values of the quasiparticle mass observed in  $\kappa$ -(BEDT-TTF)<sub>2</sub>Cu(NCS)<sub>2</sub> [1]. Hence, the changes in Fermi-surface topology may cause *both* the suppression of the superconducting transition temperature and the effective mass (see Figure 2); the causal relationship between  $T_c$  and  $m^*$  suggested in earlier works [30, 31, 32] is perhaps an oversimplification.

Support for our interpretation comes from recent millimetre-wave magnetoconductivity experiments which give information about the corrugations of the quasi-one-dimensional sheets of the Fermi surface [26] in the *interlayer* direction. It was found that the corrugations on the Fermi sheets of h8 (lower  $T_c$ ) were relatively large compared to those on the sheets of d8 (higher  $T_c$ ). This again suggests that it is primarily details of the Fermi-surface topology, and in particular its nestability, that determine  $T_c$ .

In summary, we have measured details of the Fermi-surface topology of deuterated  $\kappa$ -(BEDT-TTF)<sub>2</sub>Cu(NCS)<sub>2</sub> as a function of pressure, and compared them with equivalent measurements of the undeuterated salt. We find that the superconducting transition temperature is much more dramatically suppressed by increasing pressure in the deuterated salt. This may be linked to pressure-induced changes in the Fermi-surface topology, which occur more rapidly in the deuterated salt as the pressure is raised. Our data support models for exotic d-wave superconductivity in the organics which invoke electron-electron interactions depending on the topological properties of the Fermi surface.

The work is supported by EPSRC (UK). We should like to thank Steve Blundell and Ross McDonald for stimulating discussions.

- [1] John Singleton and Charles Mielke, *Contemp. Phys.* **43**, 150 (2002).
- [2] John Singleton, *Reports on Progress in Physics*, **63**, 1111 (2000).
- [3] J. Schmalian, *Phys. Rev. Lett.* **81** 4232 (1998).
- [4] K. Kuroki, T. Kimura, R. Arita, Y. Tanaka and Y. Matsuda, preprint cond-mat 0108506 (2001).
- [5] S. Charf fi-Kaddour, A. Ben Ali, M. Héritier and R. Bennaceur, *J. Superconductivity* **14**, 317



- (2001); R. Louati, S. Charfi-Kaddour, A. Ben Ali, R. Bennaceur and M. H eritier, *Synth. Met.* **103**, 1857 (1999); R. Louati, S. Charfi-Kaddour, A. Ben Ali, R. Bennaceur and M. Heritier, *Phys. Rev. B* **62**, 5957 (2000).
- [6] K. Kuroki and H. Aoki, *Phys. Rev. B* **60**, 3060 (1999).
- [7] Won-Min Lee, *Solid State Commun.* **106**, 601 (1998).
- [8] K. Kanoda, K. Miyagawa, A. Kawamoto, Y. Nakazawa, *Phys. Rev. B* **54** 76 (1996).
- [9] H. Mayaffre, P. Wzietek, D. J erome, C. Lenoir and P. Batail, *Phys. Rev. Lett.* **75** 4122 (1995).
- [10] S.M. de Soto, C. P. Slichter, A. M. Kini, H. H. Wang, U. Geiser and J. M. Williams, *Phys. Rev. B* **54** 16101 (1996).
- [11] S. Lefebvre, P. Wzietek, S. Brown, C. Bourbonnais, D. J erome, C. M ezi ere, M. Fourmigu e and P. Batail, *Phys. Rev. Lett.* **85** 5420 (2000).
- [12] T. Arai, K. Ichimura, K. Nomura, S. Takasaki, J. Yamada, S. Nakatsuji and H. Anzai, *Phys. Rev. B* **63** 104518 (2001).
- [13] K. Izawa, H. Yamaguchi, T. Sasaki and Y. Matsuda, *Phys. Rev. Lett.* **88**, 027002 (2002).
- [14] A. Carrington, I. J. Bonalde, R. Prozorov, R. W. Giannetta, A. M. Kini, J. Schlueter, H. H. Wang, U. Geiser and J. M. Williams, *Phys. Rev. Lett.* **83** 4172 (1999).
- [15] S. Lefebvre, P. Wzietek, S. Brown, C. Bourbonnais, D. Jerome, C. Meziere, M. Fourmigue and P. Batail, *Phys. Rev. Lett.* **85**, 5420 (2000).
- [16] J.E. Eldridge, Y. Lin, H. H. Wang, J. M. Williams and A. M. Kini, *Phys. Rev. B* **57** 597 (1998).
- [17] H. Elsinger, J. Wosnitza, S. Wanka, J. Hagel, D. Schweitzer and W. Strunz, *Phys. Rev. Lett.* **84** 6098 (2000); J. Wosnitza, *Physica C* **317-318** 98 (1999).
- [18] D. Pedron, G. Visentini, R. Bozio, J. M. Williams and J. A. Schlueter, *Physica C* **276** 1 (1997).
- [19] E. Foulques, V. G. Ivanov, C. M ezi ere and P. Batail, *Phys. Rev. B* **62** R9291 (2000).
- [20] L. Pintschovius, H. Rietschel, T. Sasaki, H. Mori, S. Tanaka, N. Toyota, M. Lang and F. Steglich, *Europhys. Lett.* **37** 627 (1997); N. Toyota, M. Lang, S. Ikeda, T. Kajitani, T. Shimazu, T. Sasaki and K. Shibata, *Synth. Met.* **86** 2009 (1997).
- [21] R. M. MacFarlane, H.J. Rosen, E.M. Engler, V.Y. Lee and R.D. Jacowicz, *Phys. Rev. B* **38**, 284 (1988).
- [22] A. M. Kini, K. D. Carlson, H. H. Wang, J. A. Schlueter, J. D. Dudek, S. A. Sirchio, U. Geiser, K. R. Lykke and J. M. Williams, *Physics C* **264** 81 (1996)
- [23] J. A. Schlueter, A. M. Kini, B. H. Ward, U. Geiser, H. H. Wang, J. Montasham, R. W. Winter, G. L. Gard, *Physica C* **351** 261 (2001).
- [24] Y. Watanabe, T. Shimazu, T. Sasaki, N. Toyota, *Synth. Met.* **86** 1917 (1997).
- [25] J.A. Schlueter, U. Geiser, unpublished data (2002).
- [26] R.S. Edwards *et al.*, submitted to *Phys. Rev. Lett.*
- [27] M. Eremets, *High Pressure Experimental Methods*, (Oxford University Press, Oxford, 1996).
- [28] John Singleton, P.A. Goddard, A. Ardavan, N. Harrison, S.J. Blundell, J.A. Schlueter and A.M. Kini, *Phys. Rev. Lett.* **88**, 037001 (2002).
- [29] N. Harrison, J. Caulfield, J. Singleton, P.H.P. Reinders, F. Herlach, W. Hayes, M. Kurmoo and P. Day, *J. Phys.: Condens. Matter* **8** 5415 (1996).
- [30] J.M. Caulfield, W. Lubczynski, F.L. Pratt, J. Singleton, D.Y.K. Ko, W. Hayes, M. Kurmoo and P. Day, *J. Phys.: Condens. Matter* **6**, 2911 (1994).
- [31] H. Weiss, M.V. Kartsovnik, W. Biberacher, E. Steep, A.G.M. Janssen and N.D. Kushch, *JETP Lett.* **66**, 202 (1997); H. Weiss, M.V. Kartsovnik, W. Biberacher, E. Steep, E. Balthes, A.G.M. Jansen, K. Andres and N.D. Kushch, *Phys. Rev. B* **59**, 12370 (1999).
- [32] J.S. Brooks, X. Chen, S.J. Klepper, S. Valfells, G.J. Athas, Y. Tanaka, T. Kinoshita, N. Kinoshita, M. Tokumoto, H. Anzai and C.C. Agosta, *Phys. Rev. B* **52**, 14457 (1995).
- [33] Recent fits of this model to de Haas-van Alphen data at ambient pressure have produced the values  $t_b = 15.6$  meV,  $t_{c1} = 24.2$  meV and  $t_{c2} = 20.3$  meV [28]. Note that these  $t$  are *effective* transfer integrals, as opposed to the bare, unrenormalised transfer integrals used in a bandstructure calculation; instead, as they are based on parameters from de Haas-van Alphen data they will

- include the effects of electron-electron and electron-phonon interactions [34].
- [34] N. Harrison, E. Rzepniewski, J. Singleton, P.J. Gee, M.M. Honold, P. Day and M. Kurmoo, *J. Phys.: Condens. Matter* **11**, 7227 (1999).
- [35] D. Pedron, R. Bozio, J.A. Schlueter, M.E. Kelly, A. M. Kini, J. M. Williams, *Synth. Met.* **103** 2220 (1999).
- [36] D. Chasseau, J. Gaultier, M. Rahal, L. Ducasse, M. Kurmoo, P. Day, *Synth. Met.* **41** 2039 (1991); M. Rahal, D. Chasseau, J. Gaultier, L. Ducasse, M. Kurmoo, P. Day, *Acta Cryst.* **B53** 159 (1997).
- [37] J. Müller, M. Lang, F. Steglich, J. A. Schlueter, A. M. Kini, U. Geiser, J. Mohtasham, R. W. Winter, G. L. Gard, T. Sasaki, N. Toyota, *Phys. Rev. B* **61** 11739 (2000).
- [38] S. Sadewasser, C. Looney, J. S. Schilling, J. A. Schlueter, J. M. Williams, P. G. Nixon, R. W. Winter, G. L. Gard, *Sol. St. Commun.* **104** 571 (1997).
- [39] Reference [37] does not distinguish between d8 and h8 samples. The pressure dependence of  $T_c$  for the d8 salt extracted from thermal expansion data [37] does not agree with the current direct measurement.